Optical Materials 61 (2016) 68–76

Contents lists available at ScienceDirect

Optical Materials

journal homepage: www.elsevier.com/locate/optmat

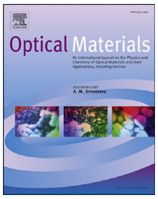

Europium(III)-doped $A_2Hf_2O_7$ (A = Y, Gd, Lu) nanoparticles: Influence of annealing temperature, europium(III) concentration and host cation on the luminescent properties

Jelena Papan [a], Dragana J. Jovanović [a], Katarina Vuković [a], Krisjanis Smits [b], Vesna Đorđević [a], Miroslav Dramićanin [a, *]

[a] *Vinča Institute of Nuclear Sciences, University of Belgrade, P.O. Box 522, 11001, Serbia*
[b] *Institute of Solid State Physics, University of Latvia, 8 Kengaraga Street, Riga, LV-1063, Latvia*

ARTICLE INFO

Article history:
Received 15 December 2015
Accepted 6 April 2016
Available online 18 May 2016

Keywords:
Rare earth hafnate
Phosphor
Luminescence
Judd-Ofelt
Europium(III)

ABSTRACT

The detailed analyses of structure and luminescence of europium(III)-doped $A_2Hf_2O_7$ (A = Y, Gd, Lu) nanoparticles is presented. Samples were prepared by time and cost effective combustion method that utilize polyethylene glycol both as a chelating agent and as a fuel, with different europium(III) concentrations (from 1 to 12 at.%), annealed at temperatures ranging from 800 to 1400 °C, and with alternating A^{3+} cation in the $A_2Hf_2O_7$ host. Then, structural variations between materials were analysed by X-ray diffraction and structural refinement, while the changes in the luminescence were assessed from the Judd-Ofelt analyses of emission spectra. Nanoparticles prepared at the lowest temperature (800 °C) had the smallest particle size of ~6 nm and showed the highest quantum efficiency when doped with 1 and 2 at.% of europium(III). Radiative transition rate and quantum efficiency of emission showed $Lu_2Hf_2O_7 > Gd_2Hf_2O_7 > Y_2Hf_2O_7$ trend.

1. Introduction

Compounds of general formula $A_2B_2O_7$, where A element is a rare earth (RE) or an element with inert lone-pair of electrons and B element is a transition metal with variable oxidation state or a post transition metal, display interesting physical properties like high melting point (~2700 K), catalytic activity, piezoelectric behaviour, ferro- and ferrimagnetism, giant magnetoresistance, and could be used as solid oxide fuel cells, dielectric materials, catalysts, immobilizers of nuclear waste and hosts for luminescent materials [1–5]. To achieve electroneutrality in these compounds, two combinations of A and B cations are possible A^{3+}/B^{4+} or A^{2+}/B^{5+}. Crystal structures of $A_2B_2O_7$ are in direct correlation with the ratio of their ionic radii, rA^{3+}/rB^{4+}. If the ratio is low ($rA^{3+}/rB^{4+} < 1.46$) they crystallize in fluorite crystal structure with $Fm\bar{3}\,m$ symmetry, where both cations are in 8-fold coordination with one anion vacancy per unit cell. In the case where $r(A^{3+})$ is larger and/or $r(B^{4+})$ is smaller, the ratio is larger ($rA^{3+}/rB^{4+} = 1.46$–1.78), and these materials crystallize in pyrochlore crystal structure with $Fd\bar{3}\,m$ symmetry, where A^{3+} is also in the 8-fold coordination while B^{4+} is in 6-fold coordination [6,7].

In the field of transition metal or lanthanide doped materials for luminescence applications, $A_2B_2O_7$ compounds activated with Mn^{4+} have been used as deep-red emitting phosphors for white LEDs [8,9], and as conventional downconversion phosphors when activated with Eu^{3+} and Sm^{3+} [10,11]. Also, these materials could be applied as scintillators due to their high density (7.93–9.95 g cm^{-3}) [12] which results in the excellent gamma-ray stopping power, and in the computer tomography and positron emission tomography [13]. Recently, luminescence thermometry with Eu^{3+} and Sm^{3+} doped $Gd_2Ti_2O_7$ has been demonstrated [14,15]. To date, only few reports have been published on the synthesis of rare earth based $A_2B_2O_7$ (A = Y, Gd, Lu; B = Ti^{4+}, Hf^{4+}, Sn^{4+}, Zr^{4+}) pyrochlores and on their luminescence when doped with trivalent rare earths, even though they are promising candidates for the activation with trivalent rare earth ions due to similarities of ionic radii and valence [16]. $Y_2Hf_2O_7$ was synthetized with a classic solid-state method, while $Gd_2Hf_2O_7$ by a vaporization method [17,18]. However, the disadvantage of these synthesis methods is the use of high temperatures (1300–1900 °C) or high pressures [18,19]. The use of soft

---

* Corresponding author.
E-mail address: dramican@vinca.rs (M. Dramićanin).

http://dx.doi.org/10.1016/j.optmat.2016.04.007
0925-3467/

chemical synthesis methods, Pechini modification of self-propagating high-temperature synthesis, co-precipitation, and combustion synthesis has yielded a cost-effective preparation of $Y_2Hf_2O_7$ [13,20,21]. Until now, properties of $Y_2Hf_2O_7$ phosphors doped with La^{3+} and Ti^{4+} ions, and $Lu_2Hf_2O_7$ doped with Tb^{3+} ions have been reported [22–24].

In this work we show time and cost effective synthesis of high-density $A_2Hf_2O_7$ nanoparticles by combustion method that utilize polyethylene glycol (PEG) both as a chelating agent and as a fuel. Then, we systematically analyse how structure of nanoparticles and emission of europium(III) ions that are introduced into nanoparticles depends on the variation of nanoparticle's composition and on the temperature of synthesis. For this purpose nanoparticles are prepared at 800, 1100 and 1400 °C, europium(III) concentration is varied between 1 and 12 at.%, and, finally, different A^{3+} cations (Y, Gd, Lu) were used for the $A_2Hf_2O_7$ host. Judd-Ofelt theory was applied for the analysis of europium(III) emission which allowed calculation and comparison of radiative and nonradiative transition rates, Judd-Ofelt intensity parameters, and quantum efficiencies.

2. Experimental

All chemicals: $HfCl_4$ (99.9%, Alfa Aesar) Y_2O_3 (99.9%, Alfa Aesar), Eu_2O_3 (99.9%, Alfa Aesar), HNO_3 (69–70%, J.T. Baker), NH_3 (30–33%, Roth) and PEG 200 (Alfa Aesar) were of the highest purity available and were used without any further purification. The direct use of $HfCl_4$ in the synthesis is undesirable because Cl^- ions could quench optical signal [25]. To eliminate Cl^- ions, $HfCl_4$ was first dissolved in water and Hf^{4+} ions formed HfO^{2+}. These ions are then transformed in $HfO(OH)_2$ in the presence of aqueous 6.7 M ammonia solution and precipitate was washed until pH value was neutral to remove access of Cl^- and NH_4^+ ions. The obtained precipitate ($HfO(OH)_2$) was used further in the synthesis after dissolution in HNO_3 acid as shown in the following three steps:

$$HfCl_4 + H_2O \rightarrow HfO^{2+} + 2H^+ + 4Cl^-$$

$$HfO^{2+} + 2NH_4OH \rightarrow HfO(OH)_2\downarrow + 2NH_4^+$$

$$HfO(OH)_2 + 4HNO_3 \rightarrow Hf(NO_3)_4 + 3H_2O$$

In the obtained $Hf(NO_3)_4$ transparent solution an appropriate amounts of Y_2O_3 and corresponding stoichiometric ratio Eu_2O_3 (x = 1, 2, 4, 8, 12 at.%) were added, and the mixture was stirred at 80 °C. After 1 h solution becomes transparent and PEG 200 was added to the solution in the 1:1 ratio (to the mass of $Y_2Hf_2O_7$). Solution was further heated at 120 °C until it formed the gel, which was then transferred to the crucible and calcined at different temperatures (T = 800, 1100 i 1400 °C) for 24 h. The europium(III)–doped $Gd_2Hf_2O_7$ and $Lu_2Hf_2O_7$ samples were obtained under identical experimental procedure and conditions.

XRD measurements were obtained using a Rigaku Smart Lab diffractometer. Diffraction data were recorded in a 2θ range from 10° to 90°, counting 0.7°/min in 0.02° steps. The structural analysis results (unit cell parameter, crystal coherence size, microstrain values, and data fit parameters) were obtained using PDXL Integrated X-ray powder diffraction software.

Luminescence measurements were obtained at room temperature with Fluorolog-3 Model FL3-221 spectrofluorometer system (Horiba JobinYvon), utilizing a 450 W Xenon lamp as an excitation source for steady-state emission measurements, and a Xenon–Mercury pulsed lamp for emission decay measurements.

Transmission electron microscopy (TEM) studies were made on a Tecnai G20 (FEI) operated at an accelerating voltage of 200 kV. Samples were supported on a perforated carbon film (S147-4, Agar scientific) and were dried in air for one day. It was observed that at a high electron radiation dose defects were induced into the crystals until their crystal structure disappeared. Therefore, for HRTEM images the electron beam intensity was reduced strongly by inserting a condenser aperture and by decreasing the spot size.

3. Results and discussion

3.1. Structure and morphology of nanoparticles

Typical HRTEM images of $Y_2Hf_2O_7$ nanoparticles doped with 2 at.% of europium(III) and annealed at different temperatures are shown in Fig. 1a, b, c. All samples reveals clear crystal structure visible in HRTEM images and also in SADP. The SADP and reconstructed electron diffraction pattern of sample annealed in 800 °C is shown Fig. 1a (right side) and corresponds to cubic structure. The crystallite sizes for sample annealed at 800 °C was in range from 3 till 7 nm, whereas for sample annealed at 1100 °C in range from 5 till 15 nm. The crystallite size distribution and average size 11.7 nm of sample annealed in 1100 °C was estimated from TEM DF images and are shown in Fig. 1b (right side) together with selected DF images. The particles of sample annealed at 1400 °C was too large to evaluate the crystallite size in TEM. All samples shows nanoparticle agglomerates with different sizes (Fig. 1c (right side)), and particle size up to 300 nm for sample annealed at 1400 °C.

Fig. 2a displays XRD patterns of the $Y_2Hf_2O_7$:2 at.% Eu^{3+} samples annealed at different temperatures (T = 800, 1100 and 1400 °C) for 24 h, while Table 1 presents structural parameters of the samples obtained after Rietveld refinement of experimental data. All patterns clearly show presence of the cubic fluorite structure ($Fm\overline{3}$ m (2 2 5)) in samples, with diffraction peaks indexed according to the ICDD 00-024-1406 card. With the increase of annealing temperature diffraction peaks became narrower and an average crystallite size of powders increases from 6 nm to 66 nm. The calculated average crystalline sizes for samples annealed at 800 °C and 1100 °C are very close to that observed in TEM images. The increase in annealing temperature did not significantly alter the unit cell parameter (*a*), therefore, the local environments around dopant europium(III) ions are similar in all samples in term of the distance between europium(III) and neighbouring ions. However, the values of microstrain are ten times lower in samples annealed at higher temperatures. XRD patterns of the $A_2Hf_2O_7$:1 at.% Eu^{3+} (A = Y, Gd, Lu) samples and structural parameters of the samples obtained after Rietveld refinement of experimental data are presented in Fig. S1. The patterns clearly show pure cubic fluorite structure (*Fmm* (2 2 5)) in the samples, with diffraction peaks indexed according to the ICDD 00-024-1406 card (for A = Y and Lu) and ICDD 00-024-0425 (for A = Gd).

Fluorite $Y_2Hf_2O_7$ crystallize in space group $Fm\overline{3}\,m(O_h^5)$ No.225, with one formula unit in the primitive cell; the basic crystallographic properties are listed in Table 2. Y^{3+} and Hf^{4+} cations randomly occupy $m\overline{3}\,m$ site, each having occupancy factor of 0.5. To maintain charge balance, there are seven oxygens and a vacancy occupying $\overline{4}\,3\,m$ site of the unit cell, as can be seen in Fig. 2b. In this type of oxygen deficient fluorite structure the occupancy for each anion site is 0.875, where any of the eight oxygen sites in the structure have an equal probability to become vacant. In Fig. 2b blue spheres represent cations, red spheres represent oxygen's, while yellow sphere is the vacancy. Blue tetrahedrons are coordination polyhedra around oxygens, yellow tetrahedron is the vacancy coordination polyhedron that also retains the shape in the crystalline structure, while coordination polyhedrons around cations are cubes as presented in red on the picture. In the 8-fold coordination, the values of ionic radii of constituting cations are: